D. W. HILLGER

INT. J. REMOTE SENSING, 1987, VOL. 8, NO. 7, 961–970

Fire detection using data from the NOAA-N satellites TOVS ?

MICHAEL MATSON and GEORGE STEPHENS

NOAA/National Environmental Satellite, Data and Information Service, Washington, D.C. 20233, U.S.A.

and JENNIFER ROBINSON

National Center for Atmospheric Research, Boulder, Colorado 80307, U.S.A.

(Received 22 July 1986; in final form 11 February 1987)

Abstract. Due to increased concern over the climatic and economic impact of fires associated with deforestation and seasonal burning, most of which occurs in remote parts of the world, it is necessary to find ways to effectively monitor such activity. The 3·8 μm channel on board the National Oceanic and Atmospheric Administration's polar-orbiting satellites is very sensitive to high temperature sources such as fires. Case studies in Mexico, Brazil, Mozambique and the Soviet Union have been selected to demonstrate the utility of this channel for fire detection. With the fire detection capability of the 3·8 μm channel and the daily global coverage, it is possible to monitor world-wide fire activity.

1. Introduction

Knowledge of regional and global fire activity is important for atmospheric, climatic and deforestation studies. Biomass burning is a major source of CO_2, CH_4, COS, NH_3, NO_x, CO, non-methane hydrocarbons, total particulates and elemental carbon particulates. Increased concentrations of these gas species and particulates have been observed during the burning seasons in Brazil (Crutzen *et al.* submitted, 1985, Greenberg and Zimmerman 1984, Greenberg *et al.* 1984) and Africa (Greenberg *et al.* 1985). CO_2 and CH_4 are both 'greenhouse' gases with long tropospheric residence times. COS and CH_4 break down in the stratosphere to sulphates and water vapour, which affect stratospheric light scattering and absorption, respectively (Crutzen 1976, Crutzen *et al.* 1979). NH_3 tends to decrease rainfall acidity while NO_x tends to increase it. Fire emissions can also markedly affect the chemical and radiative behaviour of the air mass they enter. Some effects, such as the association of reactions involving CO, CH_4, NO_x and non-methane hydrocarbons in fire emissions with major increases in tropospheric O_3 concentrations, are well documented (Fishman *et al.* 1980, Fishman *et al.* 1985). Other effects, such as a decrease in OH following burning, are strongly suggested (Hahn and Crutzen 1984). Both of these effects may be important. Tropospheric O_3 is a powerful 'greenhouse' gas (Fishman *et al.* 1979) and OH-initiated reactions provide the major pathway for transforming a large number of tropospheric compounds into their oxidized forms.

Although less well understood than gas phase effects, fire-produced aerosols may also have significant effects on the environment. Measurements of slash burns (Stith *et*

al. 1981, Radke *et al.* 1978) show production of 10^{10} to 10^{11} particles in the 0·1 to 1·0 μm range per gram of fuel burned. Burning appears to bring on a hundredfold increase in background Aitken particle counts in the atmosphere over Congolese savanna regions during the dry season (Cros *et al.* 1981). The downward arm of the Hadley Cell tends to trap smoke aerosols in the tropics in vast smog-like layers for weeks at a time. These layers may affect local radiative balances.

Fires can also have local effects on the land surface and hydrologic conditions because of the resultant destruction of vegetation. The effects include an increase in surface albedo and water runoff and a decrease in evapotranspiration. These local processes may broaden to regional scales through such processes as forest-to-grassland conversion.

Although the biogeophysical importance of regional fire activity is recognized, current fire detection methodologies are inadequate for monitoring such activity in remote areas of the world such as the tropics, northwestern Canada and Siberia. Ground-based detection systems usually suffer from limited areal coverage. The value of airborne bispectral thermal infrared sensors for improved spatial and temporal coverage of fire activity has been demonstrated (Binenko *et al.* 1974, Warren 1984). These studies find the 3–5 μm portion of the spectrum to be particularly sensitive to high temperature targets such as fires. Aircraft surveys over large areas, however, are not an economical means of operational fire detection. Several planes and many days of flying time are required to monitor active fire sites. Environmental satellites, such as the National Oceanic and Atmospheric Administration (NOAA) polar-orbiting satellites, with large swath widths, daily day and night coverage, and sensors in the 3–5 μm spectral band, offer a potential solution to the problem of efficiently and economically detecting and monitoring fires in remote areas.

2. The NOAA-N satellites

NOAA's National Environmental Satellite, Data and Information Service operates a system of polar-orbiting satellites in Sun-synchronous orbits, designated the NOAA-N series. Currently, there are two satellites in operation, NOAA-9 and NOAA-10, at an altitude of 850 km. Local equatorial crossing times are 0730 and 1930 for NOAA-10 and 1400 and 0200 for NOAA-9. Each satellite orbits the Earth 14 times a day, yielding a complete global view each day and night.

One of the primary sensors on board the NOAA-N satellites is the Advanced Very High Resolution Radiometer (AVHRR). This scanning instrument acquires data in five spectral channels, one in the visible range (0·55–0·68 μm), one in the near infrared range (0·725–1·1 μm) and three in the thermal range (3·53–3·93, 10·3–11·3 and 11·5–12·5 μm). Data are sensed by all five channels simultaneously. The three thermal channels have a minimum noise-equivalent differential temperature of 0·12 deg K for a 300 K scene and saturate at 320 K. The instrument has an instantaneous field of view of 1·4 mrad, yielding a nominal resolution of 1·1 km at nadir. At this resolution, the image swath width is 2600 km. Data acquired by the instrument are degraded on board the satellite to 4 km resolution and recorded for later transmission to one of two NOAA receiving stations, at Gilmore Creek, Alaska and Wallops Island, Virginia. This is known as the Global Area Coverage (GAC) mode of transmission. In addition, the full resolution 1·1 km data can be recorded for previously scheduled areas of the world, in the Local Area Coverage (LAC) mode, or can be received directly from the satellite by properly equipped receiving stations, in the High Resolution Picture Transmission (HRPT) mode.

3. Fire detection methodology

Matson and Dozier (1981), Matson *et al.* (1984) and Muirhead and Cracknell (1984, 1985) have demonstrated that the use of the 3·8 μm thermal infrared channel on board the NOAA polar-orbiting satellites provides the capability to detect high temperature sources such as steel plants, waste gas flares and fires. Figure 1 shows why this is so. For high temperature targets, the maximum blackbody radiance shifts away from the 11 μm channel and toward the 3·8 μm channel. Figure 2 shows a typical satellite-derived temperature plot over two high temperature sources located in Idaho. Target 1 is a small controlled forest burn and target 2 is a phosphorous plant operated by the FMC Corporation in Pocatello, Idaho. At these sources, the 3·8 μm temperatures are 16·2 deg K and 33·9 deg K higher than the corresponding 11 μm temperatures. Typical temperature differences between the two channels over land surfaces are usually 1–2 deg K. Using an algorithm developed by Matson and Dozier (1981), it is possible to use the temperature difference in the two channels to estimate the areal extent and temperature of the high temperature source causing the 3·8 μm response. For the two sources in figure 2, the area and temperature were 0·28 ha and 430 deg K for target 1, and 1·7 ha and 483 deg K for target 2. As evidenced by the calculated target sizes and the detection of the phosphorous plant, it does not take a 1·1 km target to cause a response in the 3·8 μm channel. Thus, small *subresolution* scale high temperature sources, such as fires, can be detected by the 3·8 μm channel. The size of the subresolution scale high temperature sources which can be detected depends on the target temperature and area. Although the actual lower limit of detectability is not

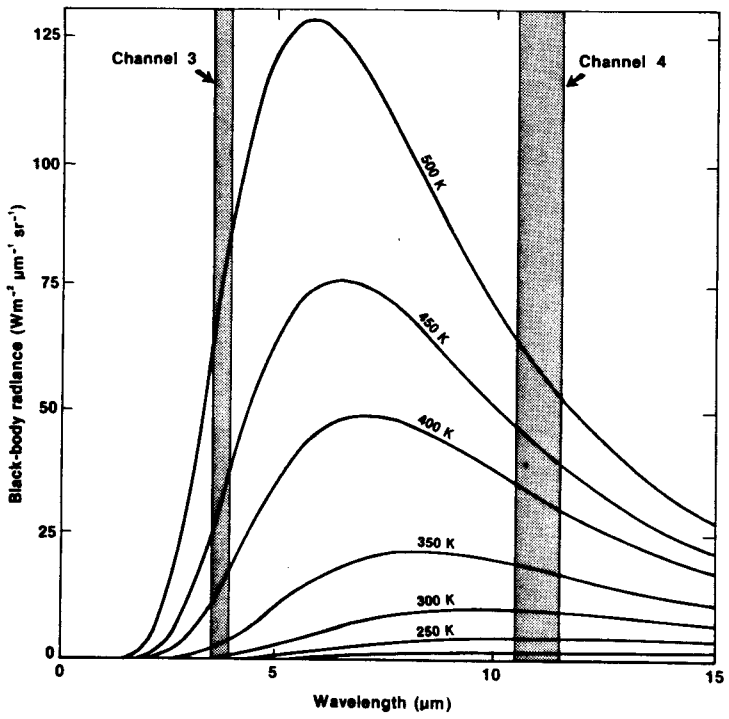

Figure 1. Planck radiances for temperatures from 200 K to 500 K. For a given increase in temperature the increase in area under the 3·8 μm segment (channel 3) of the curve is much greater than under the 11 μm segment (channel 4).

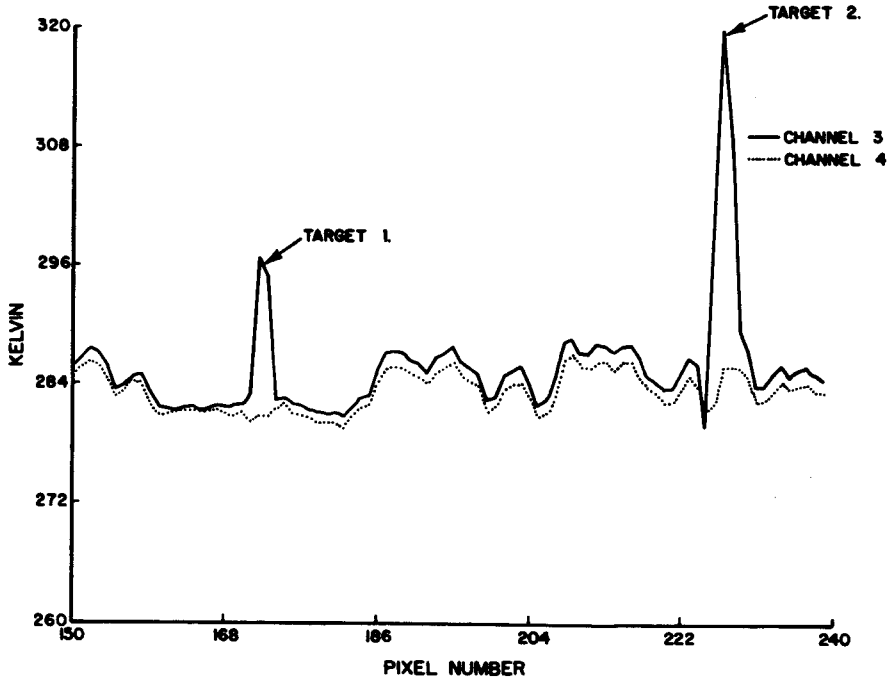

Figure 2. 3·8 μm (channel 3) and 11 μm (channel 4) brightness temperature plot of 'hot' targets 1 and 2.

known, very hot and small targets such as waste gas flares from offshore oil platforms have been detected (Matson and Dozier 1981, Muirhead and Cracknell 1984) as well as small fires from straw burning (Muirhead and Cracknell 1985).

4. Case Studies

Figure 3 is a NOAA-7 visible band image taken of southern Mexico and northern Guatemala on 18 April 1984. A number of large smoke plumes and smoke-covered areas are visible (light grey areas, labelled 'S'). Figure 4 is the 3·8 μm image of the same area. The well-defined white spots throughout the image are fires. Most of the fires seen here are associated with land clearing for agriculture. Scientists familiar with this area of Mexico have identified several distinct areas (Breedlove 1981) and the type of burning associated with each. The Grijalva Basin, the white area near the centre of the picture (labelled 'GB'), is a major agricultural centre; most of the burning here is for clearing of previously cultivated land. In contrast, the area around Veracruz, in the upper left (labelled 'V'), and the area around the Guatemala border (labelled 'G'), in the lower right, are primarily virgin forest, being cleared for agricultural use at great ecological cost. The reader should note how the 3·8 μm channel penetrates the smoke to reveal the underlying fire activity. The 3·8 μm channel radiative response is not significantly attenuated by water vapour. Smoke is largely composed of water vapour, thus the 3·8 μm channel 'sees through' the smoke.

Tucker *et al.* (1984) used NOAA-7 data taken on 9 July 1982 to identify a large (100 km by 400 km) area in Rondonia, Brazil, where massive deforestation is occurring. Figure 5 is a 3·8 μm image of this area taken on 18 August 1984. The image

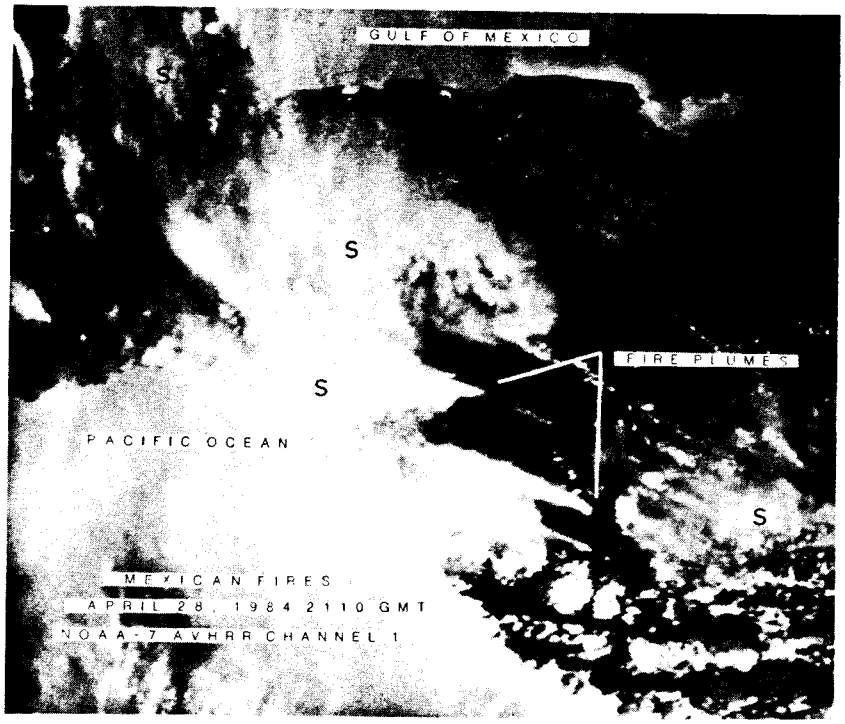

Figure 3. Visible band (0·58–0·68 μm) AVHRR image of southern Mexico and northern Guatemala on 28 April 1984. Areas labelled 'S' are smoke covered.

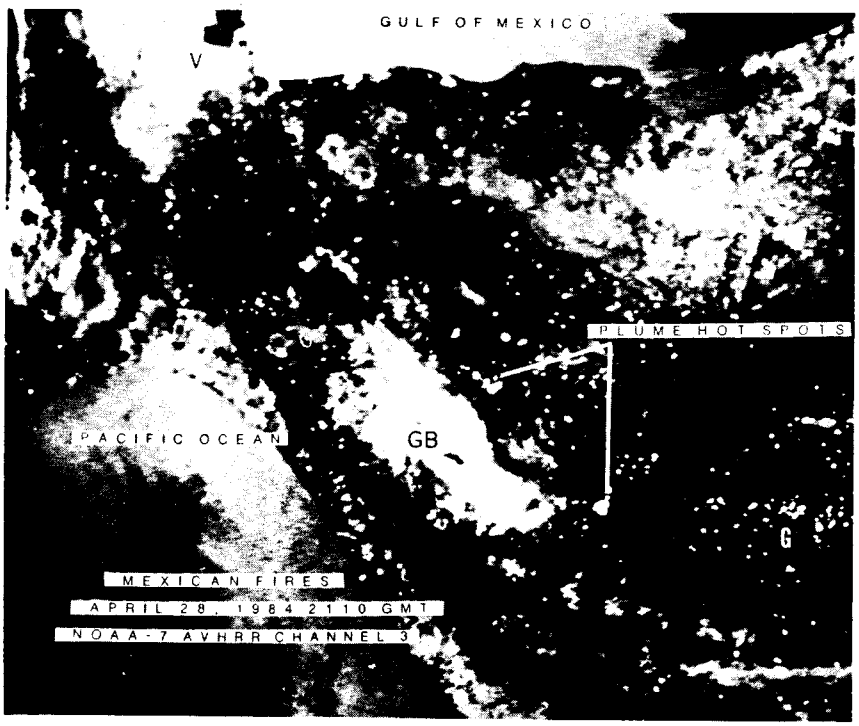

Figure 4. 3·8 μm AVHRR image of southern Mexico and northern Guatemala on 28 April 1984. Areas labelled 'GB', 'V' and 'G' refer to the Grijalva Basin, Veracruz and Guatemala portions of the image as discussed in the text.

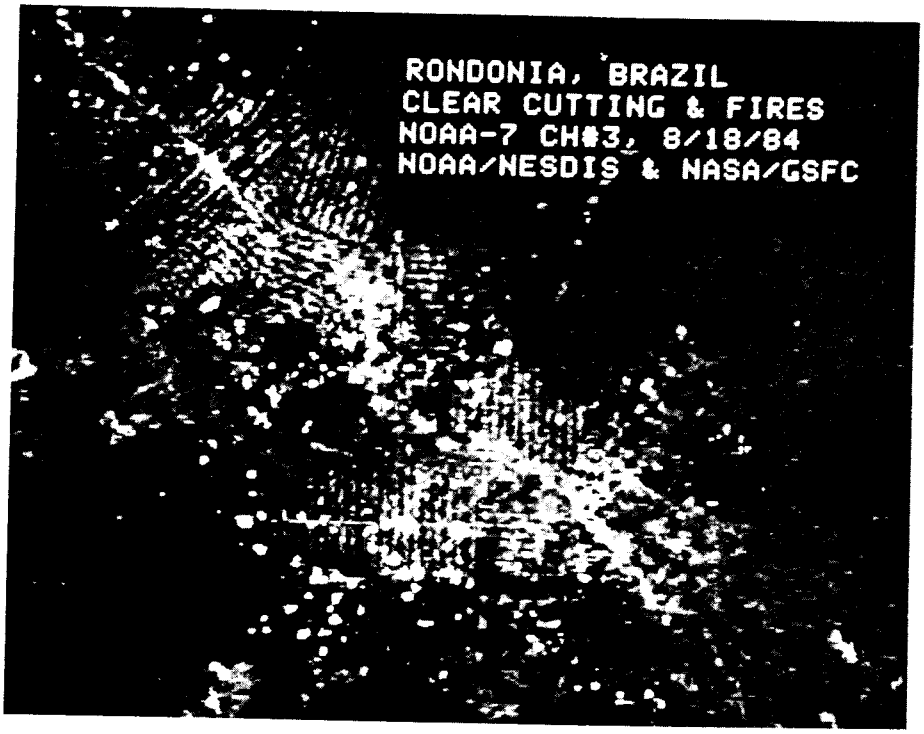

Figure 5. 3·8 μm AVHRR image of Rondonia province, Brazil, on 18 August 1984.

shows a series of warmer (grey) linear features radiating from highway BR-364 (grey, diagonal linear feature). These features were seen on the 9 July 1982 imagery and were interpreted to be large-scale, systematic forest disturbances (Tucker *et al.* 1984). A field verification mission in 1982 found the linear features to be forest-clearing swaths, some at least 80 km long, about 4 km apart, and 600 to 800 m wide. The forest clearing is part of a government-planned colonization project in which migrants are sold 100 ha lots of forest to use for agriculture or pasture (Tucker *et al.* 1984). Figure 5 also shows many 'hot spots' (white) which were not apparent on the 9 July 1982 imagery. Malingreau (personal communication) visited the area in 1986 and found that such hot spots were fires caused by slash-and-burn agriculture and continued tropical forest clearing for further colonization. On the coincident visible-band AVHRR imagery, the entire area was covered by smoke, further evidence fires were occurring in the area. The fires were not detected on the 9 July 1982 imagery because seasonal burning does not begin in this area until late July and August, when precipitation is at a minimum (Rudloff 1981). By using the 1·1 km resolution AVHRR data, it would be possible to operationally monitor the expansion of deforestation and the associated burning which is occurring in this area of Brazil.

Figure 6 is a NOAA-7 image taken over Mozambique on 26 September 1984, during a period when the country was nearing the end of a once in a 100-year drought. The image is a false colour composite of the visible, near-infrared, and 3·8 μm channels. Water is dark blue, land is green, smoke plumes are light blue and fires are red. On this one day, several hundred fires, probably associated with agricultural land clearing, appear on the image. Unfortunately, it is difficult to verify the cause of the burning due

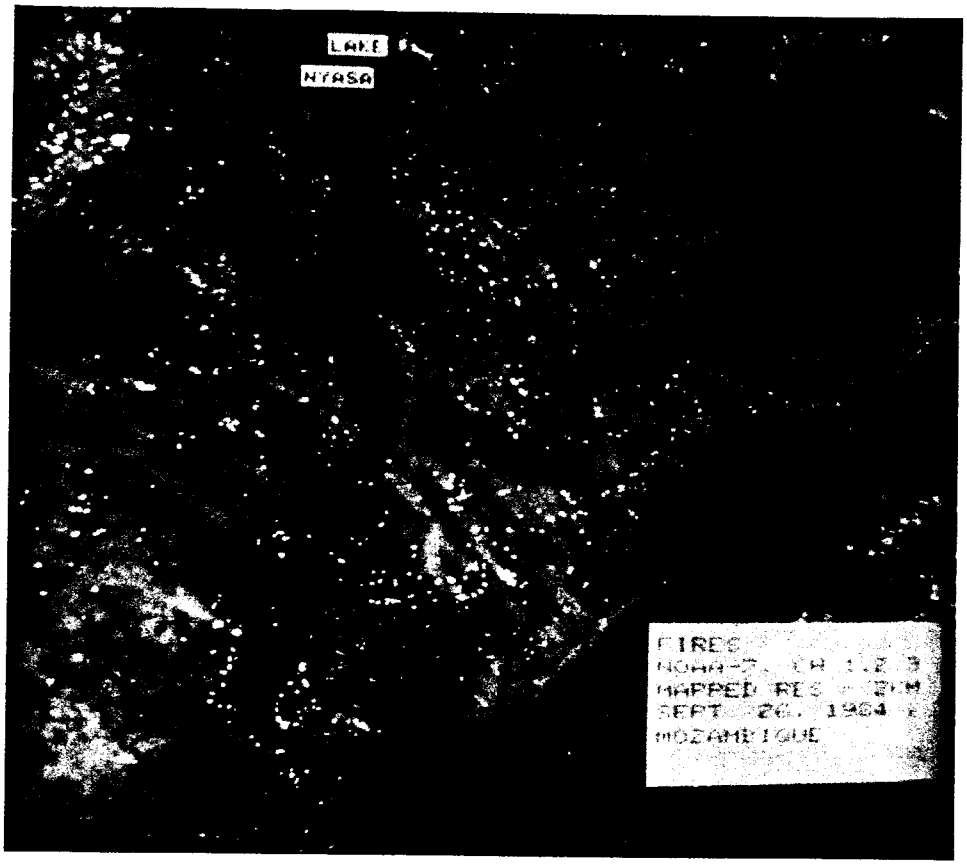

Figure 6. False colour composite AVHRR image of Mozambique, Africa, on 26 September 1984.

to the lack of field information in Mozambique. However, even in an average year September is the driest month, with the area of the country shown on the image receiving 3 mm of precipitation out of an annual mean of 600 mm (Griffiths 1972). It is during such dry months most agricultural burning occurs.

The previous case studies of fire detection have used the 1·1 km resolution data. As described earlier, the high resolution data is only available if previously scheduled for later transmission to a satellite receiving station or if the data is obtained in an area covered by such a station. To obtain operational global coverage, the data must be in the 4 km resolution GAC mode. It might seem that such a coarse resolution would be inadequate for fire detection, but as figure 7 and figure 8 show, such is not the case. Figure 7 is a NOAA-7 visible band GAC image of northern Siberia, U.S.S.R., near Yakutsk, taken on 24 July 1984. The smoke plumes (small grey streaks) between 65°N to 70°N and 105°E to 125°E are a result of lightning-induced fires in this boreal forest area. Such fires are normal for this time of year and the resulting smoke has been routinely detected on NOAA satellite visible-band imagery. Figure 8 is the coincident 3·8 μm image of the same area. The many hot spots (white) on the image are the fires associated with the plume activity in figure 7. Even at the reduced GAC resolution, the 3·8 μm channel responds to fire activity within the 4 km pixel. Malingreau *et al.* (1985)

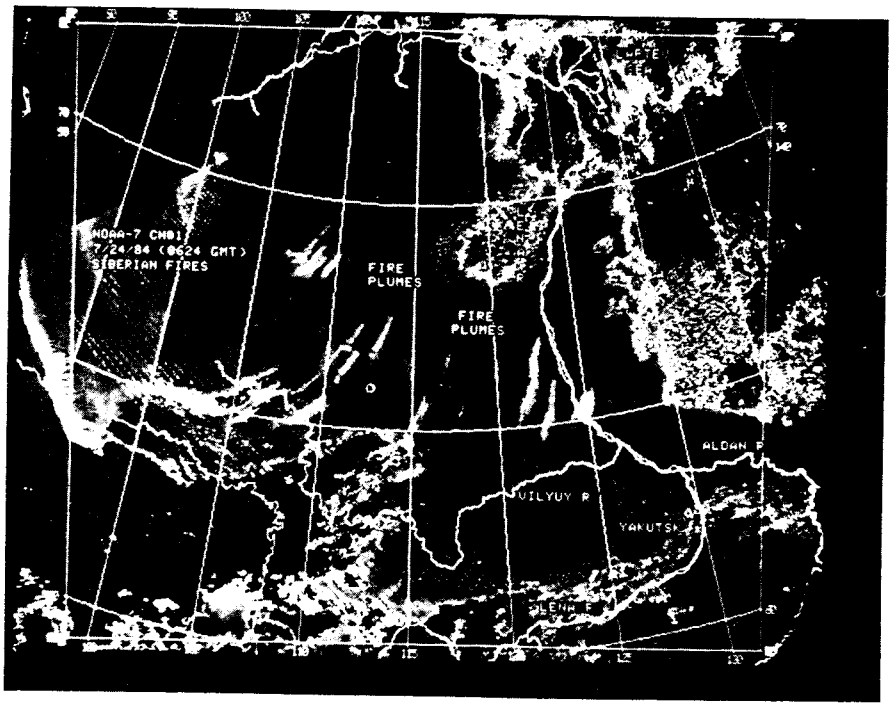

Figure 7. Visible-band (0·58–0·68 μm) AVHRR image of Siberia, U.S.S.R., on 24 July 1984.

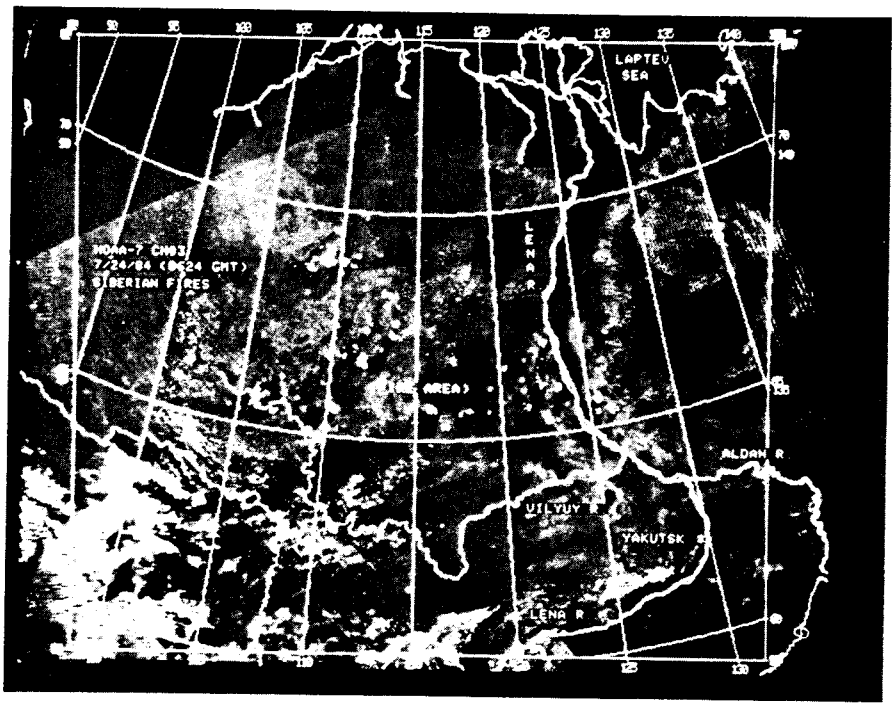

Figure 8. 3·8 μm AVHRR image of Siberia, U.S.S.R., on 24 July 1984.

have also shown this detection capability for the 1983 fires which damaged large portions of the rain forest in Kalimantan, Borneo. More case studies of fire detection using the GAC data need to be analysed to determine what size and temperature fires are detectable using the GAC data. Such studies may demonstrate the feasibility of global fire monitoring using the GAC 3·8 μm data.

5. Conclusions

In the past, operational fire detection over remote areas has been difficult, if not impossible. Many of these areas, such as in the tropics, Siberia and northwest Canada are major areas of seasonal burning. The difficulty in detecting and monitoring this burning has probably led to a serious underestimation of regional and global fire activity, affecting deforestation, the carbon dioxide cycle and atmospheric studies. The use of the 3·8 μm data from the NOAA polar-orbiting satellites offers a method of regional, and perhaps global, fire detection. This fire detection methodology could be used in conjunction with satellite-based vegetation indices (Tucker *et al.* 1985) to determine if changes in the indices are due to regional burning. In addition to fire detection related to climate studies, the 3·8 μm data can be a useful supplement to conventional fire detection techniques used in controlling fires (e.g brush and timber fires in the western United States). The few case studies presented in this report are a sample of what can be done to detect and monitor fires in the world. The satellite technology and data are available to be used by scientists interested in fire activity on any part of the Earth.

References

BINENKO, V. I., D'YACHENKO, L. N., KONDRAT'EV, K. Y., and CHERNENKO, A. P., 1974, Infrared mapping of large forest fires. In *Atmospheric Radiation Studies*, edited by K. Y. Kondrat'ev (Jerusalem: Keter Publishing House), p. 213.

BREEDLOVE, D., 1981, *Flora of Chiapas* (San Francisco: California Academy of Sciences).

CROS, B., LOPEZ, A., and FONTAN, J., 1981, Estimation of the Aitken particle source intensity in rural Equatorial Africa. *Atmos. Environment*, **15**, 83.

CRUTZEN, P. J., 1976, The possible importance of CSO for the sulphate layer of the stratosphere. *Geophys. Res. Lett.*, **2**, 73.

CRUTZEN, P. J., COFFEY, M. T., DELANY, A. C., GREENBERG, J., HAAGENSON, P., HEIDT, L., LUEB, R., MAKIN, W. G., POLLOCK, W., WARTBURG, A., and ZIMMERMAN, P. R. Observations of air composition in Brazil between the Equator and 20°S during the dry season. *Acta amazonica* (submitted).

CRUTZEN, P. J., DELANY, A. C., GREENBERG, J., HAAGENSON, P., HEIDT, L., LEUB, R., POLLOCK, W., SEILER, W., WARTBURG, A., and ZIMMERMAN, P. R., 1985, Tropospheric chemical composition measurements in Brazil during the dry season. *J. atmos. Chem.*, **2**, 233.

CRUTZEN, P. J., HEIDT, L. E., KRASNEC, J. P., POLLOCK, W. H., and SEILER, W., 1979, Biomass burning as a source of atmospheric gases CO, H_2, N_2O. *Nature, Lond.*, **282**, 253.

FISHMAN, J., MINNIS, P., and TAYLOR, M. Z., 1985, Ozone emissions from tropical forest and savannah fires from satellite observations. *Eighth Conference on Fire and Forest Meteorology* (Society of American Foresters), p. 73.

FISHMAN, J., RAMANATHAN, V., CRUTZEN, P. J., and LIU, C. S., 1979, Tropospheric ozone and climate. *Nature, Lond.*, **282**, 818.

FISHMAN, J., SEILER, W., and HAAGENSON, P., 1980, Simultaneous presence of O_3 and CO bands in the troposphere. *Tellus*, **32**, 456.

GREENBERG, J. P., and ZIMMERMAN, P. R., 1984, Non-methane hydrocarbons in remote tropical, continental and marine atmospheres. *J. geophys. Res.*, **89**, 4767.

GREENBERG, J. P., ZIMMERMAN, P. R., and CHATFIELD, R. B., 1985, Non-methane hydrocarbon and carbon monoxide concentrations in Africa savanna air. *Geophys. Res. Lett.*, **12**, 113.

GREENBERG, J. P., ZIMMERMAN, P. R., HEIDT, L., and POLLOCK, W. J., 1984, Hydrocarbon and carbon monoxide emissions from biomass burning in Brazil. *J. geophys. Res.*, **89**, 1350.

GRIFFITHS, J. F., 1972, *Climates of Africa*, edited by J. F. Griffiths (Amsterdam: Elsevier).

HAHN, J., and CRUTZEN, P. J., 1984, The role of fixed nitrogen in atmospheric photochemistry. *Phil. Trans. R. Soc.*, **296**, 521.

MALINGREAU, J. P., STEPHENS, G., and FELLOWS, L., 1985, Remote sensing of forest fires: Kalimantan and North Borneo in 1982–83. *Ambio*, **6**, 314.

MATSON, M., and DOZIER, J., 1981, Identification of subresolution high temperature sources using a thermal IR sensor. *Photogramm. Engng remote Sensing*, **47**, 1311.

MATSON, M., SCHNEIDER, S. R., ALDRIDGE, B., and SATCHWELL, B., 1984, Fire detection using the NOAA-series satellites. NOAA Technical Report NESDIS 7, Department of Commerce, Washington, D.C.

MUIRHEAD, K., and CRACKNELL, A. P., 1984, Identification of gas flares in the North Sea using satellite data. *Int. J. remote Sensing*, **5**, 199.

MUIRHEAD, K., and CRACKNELL, A. P., 1985, Straw burning over Great Britain detected by AVHRR. *Int. J. remote Sensing*, **6**, 827.

RADKE, L. F., STITH, J. L., HEGG, D. A., and HOBBS, P. V., 1978, Airborne studies of particles and gases from forest fires. *J. Air Pollut. Control Ass.*, **28**, 30.

RUDLOFF, W., 1981, *World-Climates* (Stuttgart: Wissenschaftliche Verlagsgesellschaft).

STITH, J. L., RADKE, L. F., and HOBBS, P. V., 1981, Particle emissions and the production of ozone and nitrogen oxides from the burning of forest slash. *Atmos. Environment*, **15**, 73.

TUCKER, C. J., HOLBEN, B. N., and GOFF, T. E., 1984, Intensive forest clearing in Rondonia, Brazil, as detected by satellite remote sensing. *Remote Sensing Environ.*, **15**, 255.

TUCKER, C. J., TOWNSHEND, J. R. G., and GOFF, T. E., 1985, African land-cover classification using satellite data. *Science, N.Y.*, **227**, 369.

WARREN, J. R., 1984, *Thermal Infrared Users Manual* (Washington, D.C.: Department of Agriculture).

INT. J. REMOTE SENSING, 1987, VOL. 8, NO. 7, 959

Cover

Colour infrared photograph of Mozambique, Africa, centred at the mouth of the Zambezi River and taken by crew members on the STS-41G Shuttle mission. The date of the photograph is 4 October 1984. The long white plumes are due to seasonal agricultural burning in the area, see the paper by M. Matson, G. Stephens and J. Robinson in this issue (p. 961). Photograph courtesy of NASA Johnson Space Center/Space Shuttle Earth Observations Project.